Study of the Packing Density and Molecular Orientation of Bimolecular Self-Assembled Monolayers of Aromatic and Aliphatic Organosilanes on Silica

Matthew B. Smith,[†] Kirill Efimenko,[†] Daniel A. Fischer,[‡] Simon E. Lappi,[§] Peter K. Kilpatrick,[†] and Jan Genzer*,[†]

Department of Chemical & Biomolecular Engineering, North Carolina State University, Raleigh, North Carolina 27695-7905, Ceramics Division, National Institute of Standards and Technology, Gaithersburg, Maryland 20899, Department of Chemistry, North Carolina State University, Raleigh, North Carolina 27695-8204

Received August 22, 2006

Bimolecular self-assembled monolayers (SAMs) of aromatic and aliphatic chlorosilanes were self-assembled onto silica, and their characteristics were established by contact angle measurement, near-edge X-ray absorption fine structure spectroscopy, and Fourier transform infrared spectroscopy. Three aromatic constituents (phenyltrichlorosilane, benzyltrichlorosilane, and phenethyltrichlorosilane) were studied in combination with four aliphatic coadsorbates (butyltrichlorosilane, butyldimethylchlorosilane, octadecyltrichlorosilane, and octadecyldimethylchlorosilane). Our results demonstrate that whereas SAMs made of trichlorinated organosilanes are densely packed, SAMs prepared from monochlorinated species are less dense and poorly ordered. In mixed systems, trichlorinated aromatics and trichlorinated aliphatics formed SAMs with highly tunable compositions; their surfaces were compositionally homogeneous with no large-scale domain separation. The homogeneous nature of the resulting SAM was a consequence of the formation of in-plane siloxane linkages among neighboring molecules. In contrast, when mixing monochlorinated aliphatics with trichlorinated aromatics, molecular segregation occurred. Although the two shortest aromatic species did not display significant changes in orientation upon mixing with aliphatics, the aromatic species with the longest polymethylene spacer, phenethyltrichlorosilane, displayed markedly different orientation behavior in mixtures of short- and long-chain aliphatics.

Introduction

The ability to tailor the physical and chemical properties of surfaces is of tremendous interest from both a purely scientific as well as an applied perspective. One well-known method used to modify the characteristics of material surfaces is that of molecular self-assembly of monolayer films onto reactive substrates. Two common methods involve the deposition of self-assembled monolayers (SAMs) made of thiols deposited onto noble metals (e.g., gold, silver, palladium, platinum, copper, mercury) or semiconductor surfaces (e.g., GaAs) and the self-assembly of organosilanes on oxide-containing surfaces (e.g., silica). Such SAMs have been shown to possess a high degree of structural uniformity. Through ω substitution of self-assembled alkyl chains or through substituent-group functionalization of phenyl rings, for example, it is possible to manipulate surface properties such as wettability, electrical resistivity, and chemical resistance. Achieving nanoscale control of such systems offers a wide range of potential applications including the design of nanocircuitry and the engineering of biological interfaces. The aforementioned physical properties are dictated by both the chemical nature of the newly created surfaces (dictated primarily by the ω terminus) and the degree of packing and in-plane heterogeneity of the SAMs.

Much research has been performed on both thiol- and silane-based SAMs assembled on noble metals and on silica, respectively. These films have been characterized using a variety of experimental probes including surface wettability,[1−18] IR spectroscopy,[2−4,7,10,13,14,17,19−28] ellipsometry,[2−4,6,7,10,11,13,14,17−19,23,25] cyclic voltammetry,[7,11,13,22,24,29,30] and impedance spectroscopy.[11] The most widely characterized systems involve unimolecular SAMs made of aliphatic molecules. Octadecyltrichlorosilane

* Corresponding author. E-mail: jan_genzer@ncsu.edu.
[†] Department of Chemical & Biomolecular Engineering, North Carolina State University.
[‡] National Institute of Standards and Technology.
[§] Department of Chemistry, North Carolina State University.

(1) Allara, D. L.; Parikh, A. N.; Judge, E. *J. Chem. Phys.* **1994**, *100*, 1761−1764.
(2) Allara, D. L.; Parikh, A. N.; Rondelez, F. *Langmuir* **1995**, *11*, 2357−2360.
(3) Angst, D. L.; Simmons, G. W. *Langmuir* **1991**, *7*, 2236−2242.
(4) Chang, S. C.; Chao, I.; Tao, Y. T. *J. Am. Chem. Soc.* **1994**, *116*, 6792−6805.
(5) Fadeev, A. Y.; McCarthy, T. J. *Langmuir* **1999**, *15*, 3759−3766.
(6) Fadeev, A. Y.; McCarthy, T. J. *Langmuir* **2000**, *16*, 7268−7274.
(7) Finklea, H. O.; Robinson, L. R.; Blackburn, A.; Richter, B.; Allara, D.; Bright, T. Formation*Langmuir* **1986**, *2*, 239−244.
(8) Genzer, J.; Efimenko, K. *Science* **2000**, *290*, 2130−2133.
(9) Moineau, J.; Granier, M.; Lanneau, G. F. *Langmuir* **2004**, *20*, 3202−3207.
(10) Parikh, A. N.; Allara, D. L.; Azouz, I. B.; Rondelez, F. *J. Phys. Chem.* **1994**, *98*, 7577−7590.
(11) Sabatani, E.; Cohenboulakia, J.; Bruening, M.; Rubinstein, I. *Langmuir* **1993**, *9*, 2974−2981.
(12) Szafranski, C. A.; Tanner, W.; Laibinis, P. E.; Garrell, R. L. *Langmuir* **1998**, *14*, 3570−3579.
(13) Tao, Y. T.; Wu, C. C.; Eu, J. Y.; Lin, W. L. *Langmuir* **1997**, *13*, 4018−4023.
(14) Tour, J. M.; Jones, L.; Pearson, D. L.; Lamba, J. J. S.; Burgin, T. P.; Whitesides, G. M.; Allara, D. L.; Parikh, A. N.; Atre, S. V. *J. Am. Chem. Soc.* **1995**, *117*, 9529−9534.
(15) Ulman, A.; Evans, S. D.; Shnidman, Y.; Sharma, R.; Eilers, J. E.; Chang, J. C.*J. Am. Chem. Soc.* **1991**, *113*, 1499−1506.
(16) Zhou, F.; Liu, W. M.; Xu, T.; Liu, S. J.; Chen, M.; Liu, J. X. *J. Appl. Polym. Sci.* **2004**, *92*, 1695−1701.
(17) Granier, M.; Lanneau, G. F.; Moineau, J.; Girard, P.; Ramonda, M. *Langmuir* **2003**, *19*, 2691−2695.
(18) Wang, M. J.; Liechti, K. M.; Wang, Q.; White, J. M. *Langmuir* **2005**, *21*, 1848−1857.
(19) Gun, J.; Iscovici, R.; Sagiv, J. *J. Colloid Interface Sci.* **1984**, *101*, 201−213.
(20) Hertl, W.; Hair, M. L. *J. Phys. Chem.* **1971**, *75*, 2181−2185.
(21) Creager, S. E.; Steiger, C. M. *Langmuir* **1995**, *11*, 1852−1854.
(22) Hayes, W. A.; Shannon, C. *Langmuir* **1996**, *12*, 3688−3694.

10.1021/la062475v CCC: $37.00
Published on Web 11/23/2006

(H18-TS), for example, has been shown to form well-ordered SAMs on both gold[2,7,30] and on silica.[2,3,10,17,18] Such trichlorosilanes are known to form a stabilizing cross-linked silanol network at silica surfaces.[2,3,31,32] The films produced are tightly bound to the substrate and are closely packed with low steric hindrances at the headgroup moieties. Additionally, substrate hydration has been shown to play an important role in the formation of densely packed H18-TS monolayers; chemisorbed water increases the number of surface silanol groups capable of binding silane molecules.[2,3]

Although not as widely studied as their aliphatic counterparts, SAMs made of aromatic moieties have been prepared by depositing thiol-based aryls on gold surfaces and characterized via a variety of techniques. Whereas the thiol−gold surface chemistry is certainly different from silane−silica surface chemistry, the behaviors of the two systems should nevertheless have meaningful similarities. Several groups have shown that aromatic thiols can produce well-ordered films. The presence of the aromatic moiety greatly impacts molecular ordering,[4,11−13,21,23,24,29,33,34] which may be tuned by the addition of multiple aromatic moieties[11,13,33,34] or substituent groups on the aromatic ring.[29] Tao et al.[13] and Szafranski et al.[12] both explored the effects of bond orbital hybridization at the thiolate headgroup on aromatic SAM formation. Tao et al.[13] compared the properties of SAMs of benzenethiol, benzenemethanethiol, biphenylthiol, and 4-biphenylmethane-thiol on gold. They observed that the addition of the methylene group at the mercapto moiety greatly improved the packing density and surface coverage of the films. Tao and co-workers suggested that the hybridization at the Au−S−C bond strongly affected the orientation of the thiol and thus the overall packing. Szafranski et al.[12] also studied the self-assembly of benzenethiol and benzenemethanethiol as well as that of several other aromatic thiols on gold. Their data indicated that the aromatic rings do not interact with the gold surface and that the interaction with the substrate is governed exclusively by the headgroup configuration. Sabatani et al.,[11] whose work will be discussed in more detail below, also observed poor packing of benzenethiol, which tended to lie flat against the substrate. The results of Whelan et al.,[24] who also studied SAMs of benzenethiol on gold, are somewhat at odds with the reports by others. Specifically, Whelan and co-workers observed that for long deposition times benzenethiol can form packed SAMs with molecular orientations nearly perpendicular to the substrate surface. The researchers posited that at low immersion times the molecules lay flat on the surface and the orientation subsequently changed such that the phenyl rings reoriented perpendicular to the substrate after a much slower SAM formation step.

Whereas the characteristics of single-component SAMs made of alkyl silanes on silica have been documented rather well throughout the literature, much less work has been done on systems comprising aromatic silanes. Of note, however, is the work of Dulcey et al.,[35] who investigated the use of single-component SAMs of aromatic trichlorinated silanes as a platform for lithographic imaging. Employing several aromatic trichlorosilanes of varying structural configurations, Dulcey et al. demonstrated that deep ultraviolet (DUV) radiation cleaves the aromatic moiety from the silane functionality, leaving an exposed silanol group that may undergo further chemical functionalization. Another pertinent body of work is that of Moineau et al.,[9] who studied the effects of varying the degree of aryl silane headgroup chlorination on SAM formation. Specifically, these researchers compared SAMs of phenyltrichlorosilane, phenyldichlorosilane, and phenylchlorosilane as well as those of several other aromatic silanes. They observed that the degree of chlorination had a pronounced effect on the density and thickness of the SAMs formed, with the trichlorinated species forming the densest network of surface-polymerized molecules.

Several groups have demonstrated the efficacy of tuning surface properties by forming mixed monolayers from solutions of varying composition.[22,36−38] Very little work, however, has been done on systems involving mixed aliphatics and aromatics on gold and (even less) on silica. One body of work germane to the present work, however, is that of Sabatani et al.,[11] who studied SAMs of benzenethiol, *p*-biphenyl mercaptan (BPM), and *p*-terphenyl mercaptan (TPM) on gold and in mixed systems with octadecanethiol. Their voltammetric studies demonstrated that both BPM and TPM formed reliable, well-packed single-component SAMs whereas benzenethiol did not. The benzenethiol SAMs, however, did appear to undergo the greatest structural change upon subsequent exposure to octadecanethiol. Whereas single-component SAMs of benzenethiol were unable to block the electrode reaction effectively, subsequent exposure to octadecanethiol resulted in a SAM whose electrode-blocking ability was greatly augmented, presumably because the octadecanethiol displaced or filled in gaps between loosely packed benzenethiol molecules. Also relevant is the work of Wang et al.,[39] who studied two-component SAMs of 2-mercapto-5-methyl-1,3,4-oxadiazole and dodecanethiol on gold. By controlling the surface composition through the composition of the deposition solutions, they were able to fabricate surfaces whose electrochemical permeabilities could be manipulated.

Whereas studies of SAMs made of aliphatic molecules have been widely reported throughout the literature, much less work has been done on SAM films of aromatic molecules and even less on mixed systems comprising both aromatic and aliphatic moieties. Such mixed systems, though, may potentially provide a convenient means by which to manipulate the physical and chemical properties of surfaces; by controlling the relative amounts of individual species present in a SAM as well as by controlling their chemical functionalities, it may be possible to engineer surfaces with very specific optical, electrochemical, or other physicochemical properties. Chlorosilanes adsorbed onto silica represent a logical system choice; the resulting siloxane bonds provide a viable platform for modifying just about any oxide-containing surface widely used throughout many industries. Therefore, the chief objective of this work is to study the formation

(23) Kim, C. H.; Han, S. W.; Ha, T. H.; Kim, K. ′*Langmuir* **1999**, *15*, 8399−8404.
(24) Whelan, C. M.; Smyth, M. R.; Barnes, C. J. *Langmuir* **1999**, *15*, 116−126.
(25) Brower, T. L.; Cook, M.; Ulman, A. ¢*J. Phys. Chem. B* **2003**, *107*, 11721−11725.
(26) Chaudhury, M. K.; Owen, M. J. *J. Phys. Chem.* **1993**, *97*, 5722−5726.
(27) Snyder, R. G.; Strauss, H. L.; Elliger, C. A. *J. Phys. Chem.* **1982**, *86*, 5145−5150.
(28) Wang, R. W.; Baran, G.; Wunder, S. L. *Langmuir* **2000**, *16*, 6298−6305.
(29) Nishi, N.; Hobara, D.; Yamamoto, M.; Kakiuchi, T. *Langmuir* **2003**, *19*, 6187−6192.
(30) Sabatani, E.; Rubinstein, I. *J. Phys. Chem.* **1987**, *91*, 6663−6669.
(31) Wasserman, S. R.; Tao, Y. T.; Whitesides, G. M. *Langmuir* **1989**, *5*, 1074−1087.
(32) Sagiv, J. *J. Am. Chem. Soc.* **1980**, *102*, 92−98.
(33) Dhirani, A. A.; Zehner, R. W.; Hsung, R. P.; GuyotSionnest, P.; Sita, L. R. *J. Am. Chem. Soc.* **1996**, *118*, 3319−3320.
(34) Frey, S.; Stadler, V.; Heister, K.; Eck, W.; Zharnikov, M.; Grunze, M.; Zeysing, B.; Terfort, A. *Langmuir* **2001**, *17*, 2408−2415.
(35) Dulcey, C. S.; Georger, J. H.; Chen, M. S.; McElvany, S. W.; Oferrall, C. E.; Benezra, V. I.; Calvert, J. M. *Langmuir* **1996**, *12*, 1638−1650.
(36) Kang, J. F.; Liao, S.; Jordan, R.; Ulman, A. *J. Am. Chem. Soc.* **1998**, *120*, 9662−9667.
(37) Kang, J. F.; Ulman, A.; Jordan, R.; Kurth, D. G. *Langmuir* **1999**, *15*, 5555−5559.
(38) Ulman, A. *Acc. Chem. Res.* **2001**, *34*, 855−863.
(39) Wang, Z.; Shi, Y. L.; Li, H. L. *Can. J. Chem. Rev. Can. Chim.* **2001**, *79*, 328−336.

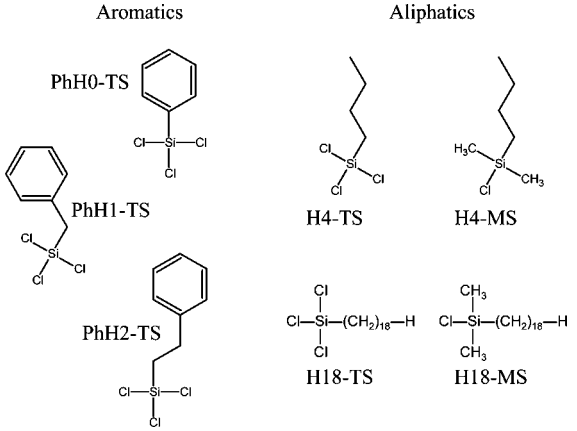

Figure 1. Silane chemical structures. The aromatics are phenyltrichlorosilane (PhH0-TS), benzyltrichlorosilane (PhH1-TS), and phenethyltrichlorosilane (PhH2-TS). The aliphatics are butyltrichlorosilane (H4-TS), butyldimethylchlorosilane (H4-MS), octadecyltrichlorosilane (H18-TS), and octadecyldimethylchlorosilane (H18-MS).

Table 1. Silane Molecules Studied and Their Nomenclature in the Current Article[a]

molecule name	nomenclature
phenyltrichlorosilane	PhH0-TS
benzyltrichlorosilane	PhH1-TS
phenethyltrichlorosilane	PhH2-TS
butyltrichlorosilane	H4-TS
butyldimethylchlorosilane	H4-MS
octadecyltrichlorosilane	H18-TS
octadecyldimethylchlorosilane	H18-MS

[a] The phenylated molecules are designated PhH*x*-TS, where *x* signifies the number of methylene spacers. The trichlorinated and monochlorinated aliphatic molecules are designated H*x*-TS and H*x*-MS, respectively, where *x* signifies the number of methyl or methylene groups.

and characteristics of mixed-silane SAMs on silica surfaces. Specifically, we will report on the preparation of mixed SAMs comprising aromatic and aliphatic silanes co-deposited from organic solutions and study their properties by a battery of surface-sensitive experimental probes including contact angle measurements, reflectance Fourier transform infrared spectroscopy (FTIR), and near-edge X-ray absorption fine structure (NEXAFS) spectroscopy. Three aromatic and four aliphatic molecules are employed; their molecular structures are presented in Figure 1. For simplicity, we reference the silane molecules using the nomenclature given in Table 1. The phenyl-based chlorosilanes are designated PhH*x*-TS, where *x* signifies the number of methylene spacers. The trichlorinated and monochlorinated aliphatic molecules are designated H*x*-TS and H*x*-MS, respectively, where *x* signifies the number of methyl and methylene groups in the alkyl chain. The aromatic species are phenyltrichlorosilane (PhH0-TS), benzyltrichlorosilane (PhH1-TS), and phenethyltrichlorosilane (PhH2-TS). Each of these three aromatics is trichlorinated and thus capable of forming in-plane cross-linked silanol networks in the vicinity of the silica surface; the molecules differ only in the length of the polymethylene (PM) spacer region between the phenyl group and the silane moiety. It is hypothesized that increasing the length of the PM spacer region should reduce the molecular rigidity and in turn increase the rotational mobility of the aromatic ring. The aliphatic species explored are butyltrichlorosilane (H4-TS), butyldimethylchlorosilane (H4-MS), octadecyltrichlorosilane (H18-TS), and octadecyldimethylchlorosilane (H18-MS). Both H4-TS and H18-TS are trichlorinated and thus capable of forming cross-linked in-plane networks among neighboring molecules. The monochlorinated aliphatics, H4-MS and H18-MS, however, are incapable of cross linking. In addition, because of the steric hindrance imposed by the presence of the two methyl groups attached to the silicon atom, these molecules are not capable of forming densely packed SAMs.

Materials and Methods

Materials. Benzyltrichlorosilane was purchased from Gelest, Inc. (Morrisville, PA). Phenyltrichlorosilane, phenethyltrichlorosilane, butyltrichlorosilane, butyldimethylchlorosilane, octadecyltrichlorosilane, and octadecyldimethylchlorosilane were purchased from Sigma-Aldrich. All organosilanes were used as received. HPLC-grade toluene was purchased from Fisher Scientific.

Sample Fabrication. Stock solutions of 1.0% (w/w) pure chlorosilane were prepared in toluene. Bimolecular solutions of varying composition were prepared volumetrically from the single-component stock solutions such that the total silane concentration was maintained at 1.0%. Assuming a negligible volume change upon mixing for dilute solutions, all fractional compositions are assumed to be by mass of total silane present (e.g. 2:8 X/Y corresponds to 0.2% X, 0.8% Y, and 99.0% toluene). To prevent solution-phase polymerization from occurring, care was taken to minimize exposure of the solutions to ambient air by thoroughly purging the solution vessels with nitrogen gas; for latter experiments (including the FTIR experiments), solutions were prepared in a nitrogen-filled glovebag. Silicon substrates were cut to sizes of approximately 1×1 cm^2. The substrates were rinsed with absolute ethanol, dried under nitrogen gas, and cleaned in an ultraviolet/ozone chamber for at least 15 min. The substrates were then immediately placed in solution for overnight deposition. After SAM deposition, the samples were washed copiously with toluene and dried under a stream of nitrogen gas.

(To demonstrate the efficacy of our film fabrication protocol, supplementary FTIR and ellipsometry experiments were carried out on films of H18-TS under varying solvent conditions. The results are presented in the accompanying Supporting Information.)

Contact Angle. The contact angle measurements on SAMs were carried out using deionized water (DIW) as the probing liquid by employing a Ramé-Hart contact angle goniometer (model 100-00). Contact angle data provide a convenient means of characterizing the surface wettabilities (and surface energies) and molecular packing densities of SAMs. Densely packed aliphatic chains should form highly hydrophobic surfaces with characteristically large DIW contact angles (e.g., 100−110°). Furthermore, the difference between the advancing and receding contact angles, the so-called contact angle hysteresis (CAH), provides information about chemical and structural heterogeneity of the surface; a CAH smaller than ≈10° is generally considered to signify a relatively uniform surface. For advancing contact angles, approximately 8 mL of deionized water were deposited onto the surface. Advancing contact angles were measured while applying positive pressure until a constant advancing contact angle was observed. Receding contact angles were similarly measured by withdrawing deionized water until a constant receding contact angle was observed. For each spot on a substrate that was characterized, approximately 10 images were captured in rapid succession and averaged to obtain a mean contact angle for that spot. At least three spots per substrate were characterized in this manner and averaged to obtain the results reported herein.

Reflectance Fourier Transform Infrared Spectroscopy. Reflectance FTIR experiments were conducted on a BioRad FTS-6000 FTIR spectrometer in Dr. Stefan Franzen's (Department of Chemistry, NCSU) laboratory for mixed systems of PhH0-TS and aliphatic H18-TS. Mirrors were placed at 70° orientation, and 1024 scans were collected and averaged for each sample for both s- and p-polarized light. The objective of conducting FTIR experiments on this system was to observe how the introduction of small amounts of the aromatic species into a system composed primarily a semicrystalline aliphatic affects the ordering of the polymethylene chains. A semicrystalline arrangement of alkyl chains should have characteristic asymmetric and symmetric methylene stretching peaks at ca. 2920 and 2850 cm^{-1}, respectively.[1,26,27] A disruption of this

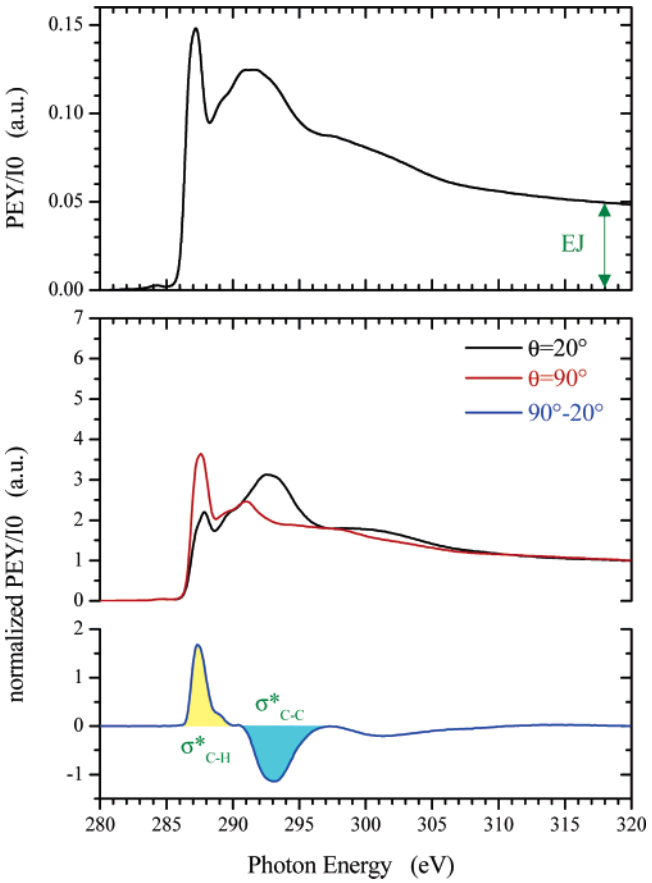

Figure 2. NEXAFS spectra of pure octadecyltrichlorosilane (H18-TS). Edge-jump (EJ) values from the 50° PEY/I0 spectra are taken to be a measure of total surface carbon (top). Difference spectra are generated by taking the difference between the normalized 90° and 20° angular spectra (bottom). Octadecyltrichlorosilane orients strongly, as is apparent from the strong angular dependence of the C−H and C−C σ* resonance peaks.

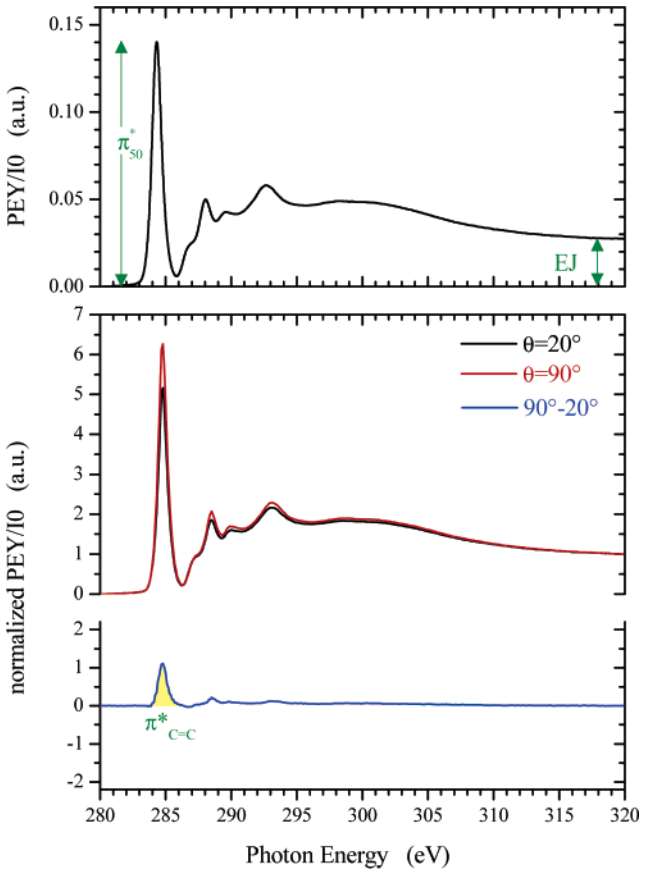

Figure 3. NEXAFS spectra of pure phenyltrichlorosilane (PhH0-TS). Edge-jump (EJ) values from the 50° PEY/I0 spectra are taken to be a measure of total surface carbon (top). Difference spectra are generated by taking the difference between the normalized 90° and 20° angular spectra (bottom). Modest orientation is observed in the π* peak (ca. 285 eV). Little orientation is observed in the C−H and C−C σ* peaks, however. Furthermore, the height of the π* peak in the normalized 50° spectra is taken to be a measure of the aromatic carbon at the surface relative to total carbon.

arrangement should result in a shift of these peaks toward a higher wavenumber.[1] H18-TS was the aliphatic compound of choice for these experiments because it is known to form a densely packed, well-ordered single-component film.

Near-Edge X-ray Absorption Fine Structure (NEXAFS) Spectroscopy. NEXAFS spectroscopy experiments were conducted at the NIST/Dow Materials Characterization Facility (beamline U7A) of the National Synchrotron Light Source at Brookhaven National Laboratory (Upton, NY). NEXAFS uses low-energy X-rays to detect bond population and the orientation of molecules on surfaces.[40] The intensity of the NEXAFS signal is a function of the density of molecules on the surface and the angle between the electric field polarization vector of the incident X-rays and the antibonding orbitals of the bonds in molecules being studied. In our work, NEXAFS is used to quantify the amounts of aromatic material and total carbonaceous material on our surfaces as well as to determine the molecular orientation of the alkyl chains and aromatic rings within our bimolecular self-assembled monolayers.

Figures 2 and 3 illustrate our analysis of carbon K-edge NEXAFS spectra. Figure 2 depicts NEXAFS spectra for an H18-TS SAM; Figure 3 presents similar data for a SAM of PhH0-TS. The "edge jump" is defined as the difference between the preedge (at 280 eV) and postedge (at 320 eV) partial electron yield signals; it is taken to be a measure of the total carbon detected (top panel). By assuming that our SAMs are sufficiently thin that the entire depth of the films is probed, we may then consider the edge jump to be related to the surface density of carbon (per unit area of the X-ray beam spot, ~0.5 mm^2) on the surface. We normalize the NEXAFS spectra by shifting the preedge values to zero and scaling the resulting postedge values to unity (middle panel). The orientation is readily visible by comparing normalized angular spectra, especially for the H18-TS, which forms a highly ordered semicrystalline SAM (Figure 2, middle panel). Difference spectra (bottom panel) may be generated to elucidate molecular orientation by subtracting the spectra taken at normal incidence ($\theta = 90°$) and glancing incidence ($\theta = 20°$) orientations, where θ is the angle between the beam and the sample surface. The orientation of aliphatic chains is observed by exploring angular dependencies of the C−H and C−C σ* resonance peaks (ca. 288 and 293 eV, respectively; cf. Figure 2). Similarly, the presence and orientation of aromatic moieties is determined from the C=C π* resonance peak at ca. 285 eV (cf. Figure 3). The NEXAFS signal collected at $\theta = 50°$ is close to the magic angle, a geometry in which the signal is independent of the molecular orientation.[40] Additionally, the height of the normalized π* peak is taken to be a measure of the amount of aromatic material relative to total carbonaceous material at the surface. Care was taken not to damage the SAMs with the X-ray beam. We have avoided this by collecting the NEXAFS spectra from a fresh position on the sample. Moreover, for a few specimens, we have rerun at least two additional scans on the very same position on the sample; in these cases in which we repeated the scans, the spectra overlapped almost perfectly, and we thus concluded that no damage occurred to the SAM. One of the drawbacks of the NEXAFS measurements is that the Auger electron detector sensitivity decays constantly with increasing time. This precluded us from comparing directly and unambiguously absolute NEXAFS intensities collected from samples in measurements performed several months apart. To

(40) Stöhr, J. *NEXAFS Spectroscopy*; Gomer, R., Ed.; Springer Series in Surface Science 25; Springer-Verlag: New York, 1992; p 403.

Table 2. Pure-Component Advancing and Receding Contact Angles and the Contact Angle Hysteresis Measured Using Deionized Water for PhH0-TS and the Four Aliphatic Silanes

	contact angle/deg		
species	advancing	receding	hysteresis
PhH0-TS	80.1	63.7	16.4
H4-TS	108.3	85.9	22.4
H4-MS	92.6	80.1	12.5
H18-TS	109.0	96.4	12.6
H18-MS	89.2	77.0	12.2

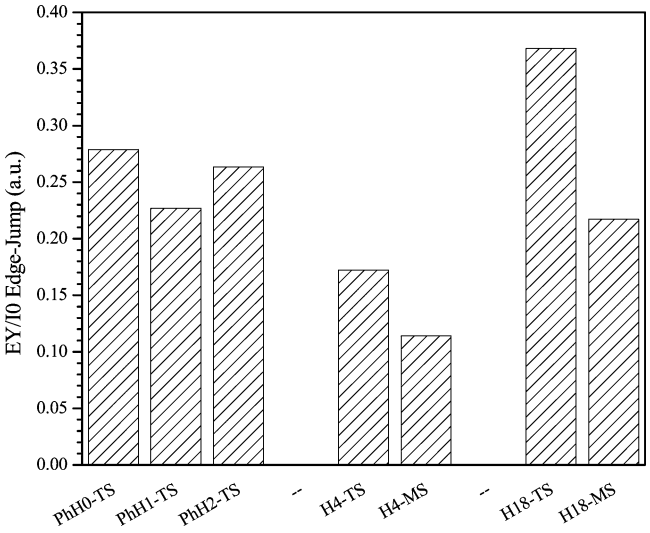

Figure 4. Average 280−320 eV EY/I0 edge-jump values for single-component systems.

appreciate the scatter caused by these effects, in the NEXAFS data we list the times at which each of the data points was taken.

Results and Discussion

Contact Angle on Single-Component Films. Contact angle data were collected for systems of PhH0-TS mixed with each of the four aliphatic species. The contact angles of the single-component films are summarized in Table 2. Several observations are immediately apparent from the single-component SAM contact angle data. Both the advancing and receding contact angles are substantially higher for systems of pure trichlorinated aliphatics (H4-TS and H18-TS) than for SAMs of either of the pure monochlorinated aliphatics. This contrast in the contact angles of trichlorinated and monochlorinated species indicates that the alkyl chain packing is strongly influenced by the headgroup configuration, similar to what has been reported earlier for semifluorinated organosilanes.[41] As argued by Genzer and co-workers,[41] the two bulky methyl groups on the monochlorinated species prevent close packing at the headgroups and, consequently, of the polymethylene chains. Only SAMs made of H18-TS display both a high advancing contact angle and a relatively low contact angle hysteresis (CAH); this confirms that the H18-TS molecules form densely packed and structurally homogeneous SAMs. Whereas the H4-TS displays a high advancing contact angle, indicating dense surface packing, it also displays the greatest CAH, revealing that the H4-TS moieties possess "structurally rough" surfaces. The alkyl chains of H4-TS are too short for van der Waals forces between neighboring molecules to effect bulk ordering.[1,26,27]

NEXAFS on Single-Component Films. Figure 4 presents the NEXAFS edge-jump values for both the aromatic and aliphatic

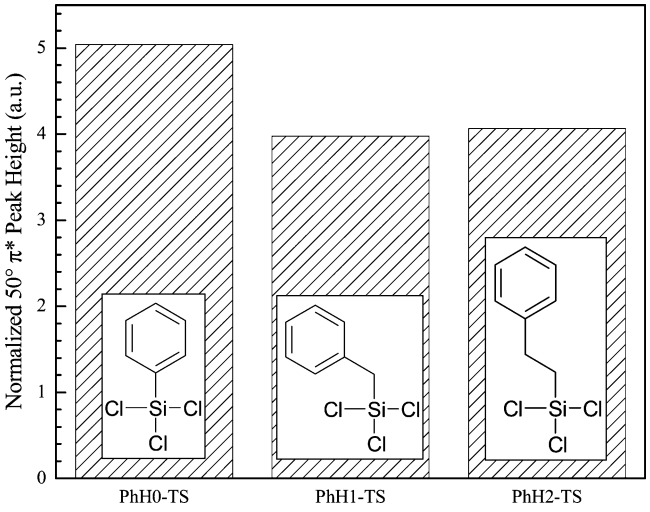

Figure 5. Normalized π^* peak heights for single-component aromatic systems.

single-component systems. Additionally, the data in Figure 5 depict the normalized π^* resonance peak height intensities for single-component aromatic systems obtained from NEXAFS spectroscopy measurements. As stated earlier, the normalized π^* peak heights provide a measure of the amount of aromatic material relative to total carbonaceous material. The data in Figure 5 show that SAMs of PhH0-TS possess a greater normalized π^* peak intensity than either PhH1-TS or PhH2-TS, whose magnitudes are comparable. Our films are sufficiently thin that NEXAFS should probe their entire depth;[42] therefore, the edge-jump data are expected to be a function of both the lateral packing density of surface molecules and film thickness. From the data in Figure 4, the edge jump decreases in the following manner: PhH0-TS > PhH2-TS > PhH1-TS. This suggests that PhH0-TS forms the most densely packed network of single-component aromatics and PhH1-TS the least. It is of particular interest that this trend of decreasing packing density does not correlate directly with an increasing number of methylene units in the chlorosilanes. By considering the aromatic-component edge-jump data together with the trend observed in π^* peak height data, it stands to reason that aromatic PhH0-TS forms a densely packed network in which the aromatic moieties are forced to assume an orientation more or less perpendicular to the surface. The lower edge-jump values for PhH1-TS and PhH2-TS, considered with these molecules' lower π^* peak intensities, suggest that the additional methylene groups drive down the normalized π^* peak intensity by contributing to the overall (nonaromatic) carbon response. Therefore, because the PhH0-TS SAM produces the most intense edge jump, despite the fact that the PhH0-TS molecule also possesses the fewest carbon atoms, we deduce that the lateral packing density of the PhH0-TS SAM is substantially higher than that of either of the longer aromatics' SAMs. The fact that the methylene groups are detected in a less densely packed arrangement for SAMs of PhH1-TS and PhH2-TS indicates that these molecules' aromatic moieties are probably oriented at more of a tilt relative to the surface normal than are those of PhH0-TS. The degree to which PhH1-TS's edge-jump signal, in particular, is lower than either of the other two aromatics' suggests that the phenyl rings in PhH1-TS are forced to assume a strong tilt, which prevents close packing and ordering through $\pi-\pi$ interactions of neighboring phenyl moieties. This is posited to be a consequence of the bond angle at the lone sp^3-hybridized

(41) Genzer, J.; Efimenko, K.; Fischer, D. A. *Langmuir* **2002**, *18*, 9307−9311.

(42) Genzer, J.; Kramer, E. J.; Fischer, D. A. *J. Appl. Phys.* **2002**, *92*, 7070−7079.

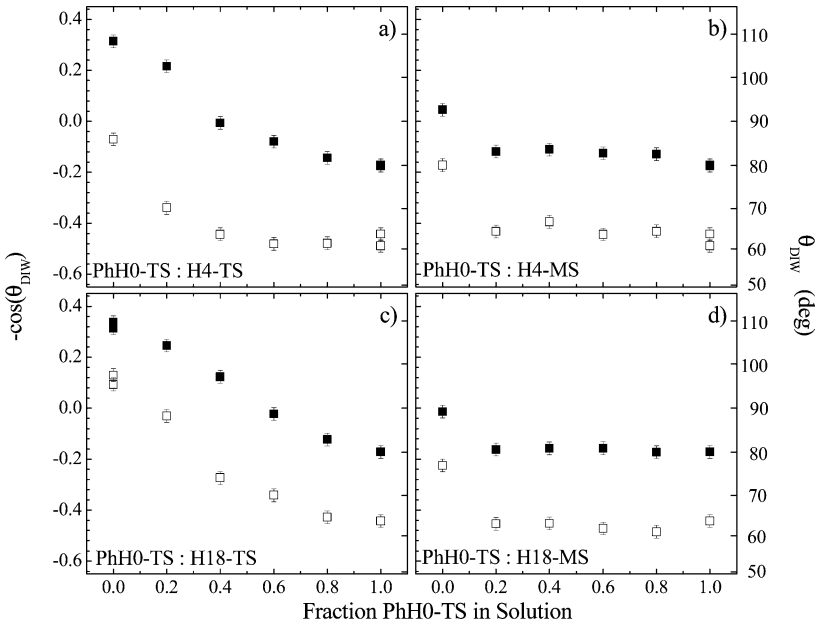

Figure 6. Negative cosine of the DI water contact angle (left ordinate) and the contact angle (right ordinate) as a function of the fraction of PhH0-TS in the liquid mixture for four different aromatic/aliphatic mixtures: (a) PhH0-TS/H4-TS, (b) PhH0-TS/H4-MS, (c) PhH0-TS/H18-TS, and (d) PhH0-TS/H18-MS. Both advancing (■) and receding (□) angles are shown. The error bars are determined from three separate measurements on each sample.

methylene spacer. By inserting just one additional methylene unit between silicon and phenyl, these structural constraints are somehow relieved, which leads to a more densely packed SAM and a more perpendicular orientation of the phenyl group, as indicated by the significantly higher edge-jump value for PhH2-TS relative to that for PhH1-TS.

The NEXAFS edge-jump data for the four aliphatic species are consistent with those obtained from contact angle measurements on single-component films (cf. Table 2). The edge-jump values of each of the two trichlorinated aliphatics are greater than those of their corresponding monochlorinated analogues. This decreased edge-jump intensity for the monochlorinated aliphatics is presumed to be primarily a consequence of reduced lateral packing of the headgroups. Reduced packing at the headgroups is expected to have the subsequent effect of reducing the overall thickness (and hence the number of carbon atoms per unit area) of the SAM. The difference in NEXAFS signal intensity between the long- and short-chain counterparts is presumed to be primarily a consequence of the film thickness differences rather than any differences in lateral packing density.

Because the difference in signal intensity between the long- and short-chain analogues is not in direct proportion to their respective numbers of carbon atoms, we believe that some of the EY/I0 signal in the short aliphatic SAM spectra is the contribution of adventitious carbon. These observations illustrate one of the principal difficulties of conducting NEXAFS on extremely thin films: it is often difficult, if not impossible, to remove all trace organics from the substrate. Thus, for extremely thin films (e.g., those of H4-TS), great care must be taken to differentiate between the signal contributions of the desired and undesired surface adsorbates. We believe any actual amount of adventitious carbon in our systems to be sufficiently small that our qualitative analysis of the NEXAFS data presented herein is still valid.

Contact Angle on Mixed Films. The advancing and receding contact angle data for mixed systems of PhH0-TS with each of the four aliphatics are presented as closed and open symbols, respectively, in Figure 6. For the mixed systems, the CAH is fairly consistent over the whole range of systems and compositions explored. There does, however, appear to be a noticeable increase in CAH for mixed systems involving either of the two trichlorinated aliphatics, indicating that these mixed systems result in structurally heterogeneous SAMs. This localized heterogeneity of mixed systems is consistent with uniform blending of the aromatic and aliphatic components in the case of trichlorinated headgroups.

To gain more insight into the structure of the mixed SAM, we estimated their surface compositions by using the Cassie−Baxter model[15]

$$\cos(\Theta_{mix}) = \varphi_1 \cos(\Theta_1) + \varphi_2 \cos(\Theta_2) \qquad (1)$$

where Θ_{mix} is the contact angle of a mixed SAM and φ_i represents the areal density of component *i* having a pure component contact angle Θ_i. From this model, the surface fractions may be calculated as

$$\varphi_1 = \frac{\cos(\Theta_{mix}) - \cos(\Theta_2)}{\cos(\Theta_1) - \cos(\Theta_2)} \qquad (2)$$

In Figure 7, we plot the fraction of PhH0-TS on the surface as a function of its fraction in the SAM toluene solution. The solid line in Figure 7 denotes the situation where the SAM composition on the surface equals that in the liquid mixture. From the data presented in Figure 7, we conclude that the mixed bimolecular SAMs can be divided roughly in two groups based on the nature of the headgroup present in the silane molecules. Mixtures of PhH0-TS with the two trichlorinated aliphatics (H4-TS and H18-TS, shown in Figure 7a,c, respectively) exhibit surface compositions that are very closely correlated with those in the solution. In this case, the trichlorinated headgroups of both the aliphatic and aromatic species can participate in polysiloxane cross linking, locking the molecules into place. Although is it difficult to conclude whether this happens in the solution before the molecules get deposited onto the substrate or only after physisorption, it is clear that PhH0-TS intermixes rather well with the H*x*-TS moieties. This assertion is further supported by the relatively small CAH (particularly for the PhH0-TS/H18-TS couple) shown in Figure 6. The close correlation between the surface and solution

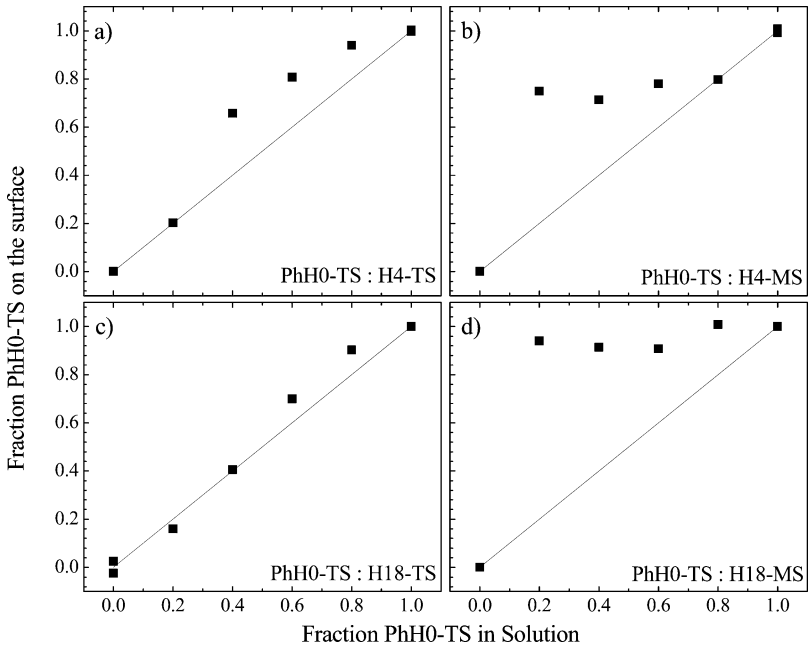

Figure 7. Fraction of PhH0-TS on the surface as a function of the fraction of PhH0-TS in the liquid mixture for four different aromatic/aliphatic mixtures: (a) PhH0-TS/H4-TS, (b) PhH0-TS/H4-MS, (c) PhH0-TS/H18-TS, and (d) PhH0-TS/H18-MS evaluated from the contact angle data shown in Figure 6 using the Cassie model (■). The solid lines denote situations where the concentration of PhH0-TS on the surface equals that in the liquid mixture.

compositions seen in mixtures of trichlorinated aliphatics and aromatic silanes contrasts sharply with the behavior observed for the systems involving a mixture of PhH0-TS with monochlorinated aliphatics. Specifically, in mixtures of PhH0-TS with either H4-MS or H18-MS (cf. Figure 7b,d) a small addition of PhH0-TS to the solution results in a rather sharp increase in the surface concentration of this species. A further increase of the amount of PhH0-TS in solution does not alter the surface composition substantially. This large disproportionality between the surface and bulk concentrations of the SAM mixture toward primarily PhH0-TS indicates that, relative to the monochlorinated aliphatics, the trichlorinated aromatic moieties adsorb to and incorporate into the surface much more aggressively by forming cross-linked polysiloxane networks. Additionally, the aforementioned steric hindrances of the methyl groups on the monochlorinated aliphatics prevent the monochlorinated species from achieving a high headgroup surface density, which results in poor packing of the aliphatic chains.

Although our reported results are for mixed systems of aromatic and aliphatic constituents only, we do not believe that the mixing properties discussed here are necessarily peculiar to mixtures of aromatic and aliphatic silanes. For example, we suspect that bimolecular films comprising both short- and long-chain aliphatics (rather than aromatics) should display similar mixing behaviors as well as a disruption of long-chain ordering. Furthermore, in such systems, we suspect the surface composition would be controlled primarily by the headgroup configurations. Mixtures of trichlorinated aliphatic silanes should produce uniformly mixed SAMs rather than segregated domains.

NEXAFS on Mixed Films. Figure 8 presents the normalized $\theta = 50°$ π^* resonance peak intensities for mixed systems of PhH0-TS with each of the four aliphatics. Recall that the normalized $\theta = 50°$ π^* resonance peak height is a measure of the amount of aromatic carbon present on the surface. Although not presented here, the major features of the mixed systems involving PhH1-TS and PhH2-TS are similar to those observed for the PhH0-TS systems. Those data are available in the accompanying Supporting Information. Some obvious trends immediately emerge from the $\theta = 50°$ π^* resonance peak intensity data. In the cases of aromatics mixed with trichlorinated aliphatics (H4-TS and H18-TS; cf. Figure 8), there is a gradual increase in the π^* resonance peak intensities as the mass content of aromatic species is increased in the deposition solution. This gradual transition is observed for each of the three aromatic species explored. It is interesting, however, that H4-TS produces a slightly different trend in mixed systems with PhH2-TS than in mixed systems with either PhH0-TS or PhH1-TS. This effect most likely indicates that PhH2-TS adsorbs to the surface less aggressively than either of the other two aromatics. Additionally, the mixed systems of H18-TS with PhH1-TS display a slightly different curvature than those of either PhH0-TS or PhH2-TS, which are very similar. Whereas mixtures of PhH0-TS and PhH2-TS with H18-TS produce surface compositions that gradually vary with solution composition, the mixtures with PhH1-TS produce a more convex trend, which falls above the diagonal parity line. Thus, in mixed solutions of PhH1-TS and H18-TS, the surface composition remains tunable but is preferentially aromatic. Note that the close correlation between the concentration of the phenyl-based chlorosilane with that in the liquid mixture observed with NEXAFS agrees with the contact angle measurements (cf. Figure 8).

For mixtures of any of the three aromatic species with monochlorinated aliphatics, the π^* resonance peak heights plateau at a value close to that for single-component systems of the aromatic species. Again, these trends are consistent with the contact angle data obtained for systems containing PhH0-TS. NEXAFS spectroscopy thus provides additional verification of the fact that, whereas monochlorinated aliphatics are incapable of adsorbing competitively to the silica surface in systems of trichlorinated aromatics, mixing two trichlorosilanes leads to SAMs that are in-plane homogeneous, at least on the length scales probed with the two methods.

One of the great benefits of using NEXAFS spectroscopy is that in addition to the concentration of a given element (i.e., from the edge jump) and a particular chemical moiety (e.g., aromatic carbon) on the surfaces one can learn about the molecular

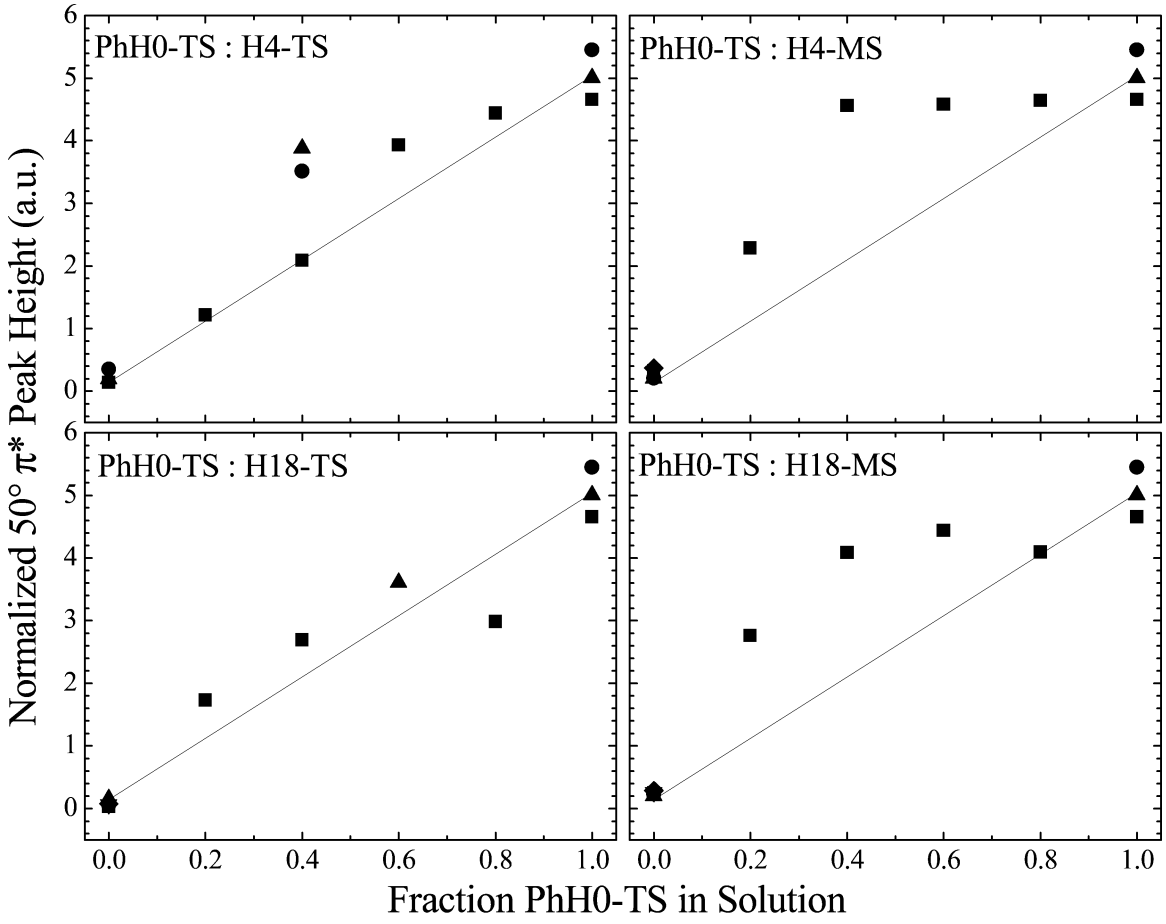

Figure 8. π^* peak heights at 50° for systems containing phenyltrichlorosilane (PhH0-TS). Data are presented from several trials: June 2004 (■), June 2005 (●, ▲), and September 2005 (▼, ◆).

orientation of selected bonds and hence gain insight into the overall orientation of the entire molecule. To do so, NEXAFS measurements must be performed at various angles between the sample and the X-ray beam. The intensity of a given bond measured with NEXAFS hence represents a contribution due to the absolute population of the bond on the surface and the orientation. One notable exception includes collecting NEXAFS data at the so-called magic angle of $\theta = 50°$, in which the signal is independent of the molecular orientation. A strong NEXAFS signal is observed when the bond's antibonding orbital is parallel to the electric vector of the polarized X-ray beam. Hence for σ bonds, whose antibonding orbitals (σ^*) lie parallel to the bond direction, a strong NEXAFS signal will be observed when the incident beam is perpendicular to the bond. In contrast, π bonds have their antibonding orbitals (π^*) oriented perpendicularly to the bond. In the latter case, the strongest NEXAFS signal is hence obtained when the bond is aligned with the incident X-ray beam. A convenient way of determining the degree of orientation is based on collecting the NEXAFS data at so-called normal incident ($\theta = 90°$) and glancing incident ($\theta = 20°$) orientations, where θ is the angle between the beam and the sample normal (or alternatively between the direction of the electric vector of the X-ray beam and the sample normal) and taking the difference between the two spectra. In Figures 2 and 3, we presented both the individual NEXAFS spectra collected at $\theta = 90°$ and 20° as well as the difference 90° − 20° for H18-TS and PhH0-TS, respectively. The intensities of the peaks in the difference plots represent a measure of the orientation of the particular bonds σ^*_{C-H} and σ^*_{C-C} for C−H and C−C bonds (cf. Figure 2) and $\pi^*_{C=C}$ for the C═C bonds in the phenyl ring (cf. Figure 3). We will use this difference as a measure of the molecular orientation in our mixed SAMs.

In Figure 9, we plot the normalized 90° − 20° $\pi^*_{C=C}$ (left ordinate) and σ^*_{C-H} (right ordinate) peak height difference data for mixtures involving the two trichlorinated aliphatics, H4-TS and H18-TS. From the 90° − 20° σ^*_{C-H} data, we see clearly that H18-TS is the only molecule that forms strongly oriented alkyl chains in single-component films. The long alkyl chains, silanol cross linking, and low steric effects at the silanol headgroups permit close packing, which leads to an almost perpendicular orientation of the polymethylene tails on the substrate. The addition of the two methyl groups at the silane atom in H18-MS disrupts the orientation of the alkyl chains (Supporting Information), presumably by limiting the molecules' packing efficiency and preventing silanol cross linking. Additionally, neither of the short aliphatics (H4-TS and H4-MS) is sufficiently long to permit strong orientation in the alkyl region.

From the 90° − 20° $\pi^*_{C=C}$ data, we conclude that all three aromatic species exhibit at least modest orientation of the phenyl moiety in single-component films. Both PhH0-TS and PhH2-TS display much stronger orientation than does PhH1-TS. Thus, the observed trend in π^* orientation does not correlate directly with an increase in methylene spacers. In fact, the trend in order as indicated by 90° − 20° $\pi^*_{C=C}$ data is identical to the trends in edge jump and in π^* peak height (cf. Figures 4 and 5). Thus, PhH0-TS has the greatest packing density and orientational order, PhH2-TS is second, and PhH1-TS has the lowest packing density and orientational order. Again, this is likely due to the very constrained bond angle in PhH1-TS that causes it to tilt such that the aromatic moiety is closer to the silicon substrate, whereas

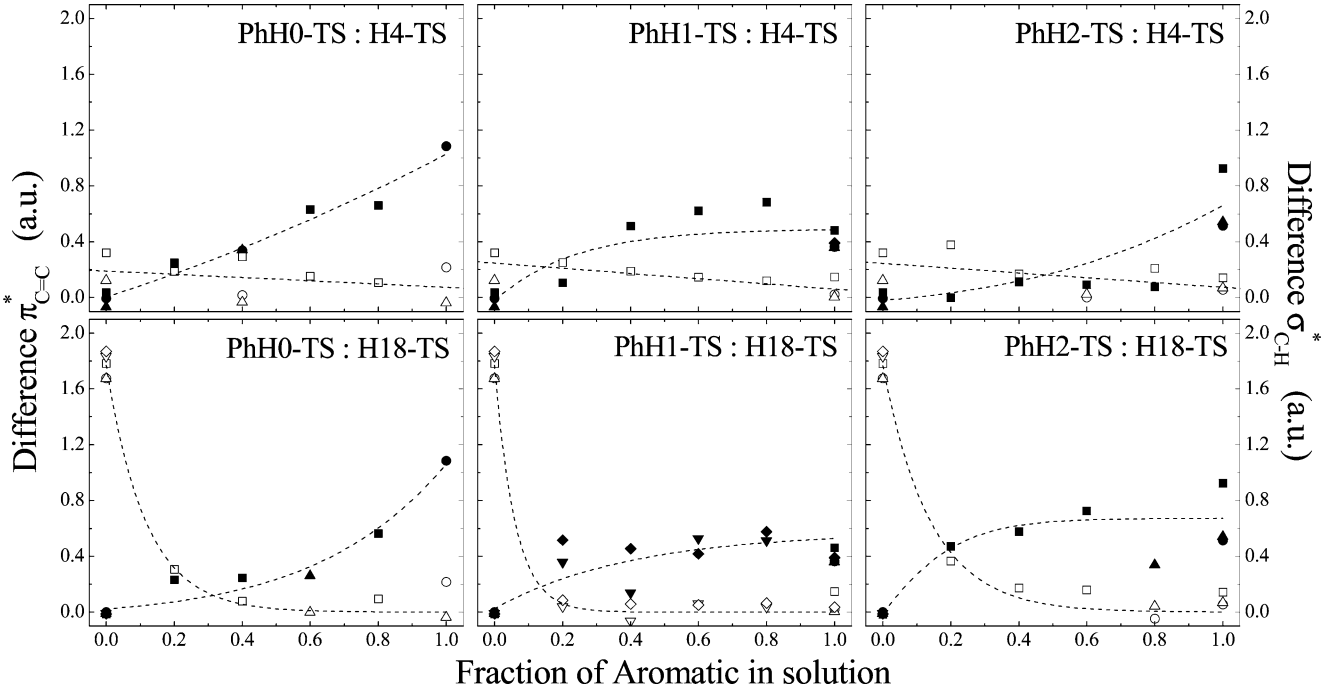

Figure 9. C−C π^* (closed symbols) and C−H σ^* (open symbols) 90° − 20° difference values for systems containing trichlorinated aliphatics. Data are presented from several trials: June 2004 (□), June 2005 (○, △), and September 2005 (▽, ◇).

with PhH0-TS and PhH2-TS, the aromatic moiety is much closer to perpendicular to the surface. We posit that the sp^3 hybridization at the methylene moiety forces PhH1-TS's aromatic ring to assume an angular tilt with respect to the surface normal that prevents close packing and the formation of ordered domains through $\pi-\pi$ interactions.

Upon comparison of the three mixed systems containing H18-TS, we detect that the apparent orientation in the σ^*_{C-H} peaks is greatly disrupted in mixtures with any one of the three aromatic species, even at relatively low aromatic content. At the lowest aromatic fraction investigated (20%), however, there does appear to be a detectable transition in alkyl chain ordering. Specifically, for the 2:8 mixtures of either PhH0-TS or PhH2-TS with H18-TS, we observe a measurable degree of orientation of the alkyl chains. For the PhH1-TS system, however, we do not observe any significant orientation in the 2:8 mixture. This exclusion of the aliphatic in systems of PhH1-TS is consistent with our assumption of a highly tilted phenyl moiety, discussed above, in which the steric effects of tilted phenyl rings inhibit the adsorption and ordering of aliphatic molecules. Furthermore, these trends in observed orientation for the 2:8 mixtures of H18-TS are consistent with those observed in the normalized 50° π^* peak height data discussed previously (cf. Figure 8).

We now focus our discussion on the effects of the aliphatic species on the ordering of aromatic moieties in mixed systems. From Figure 9, we observe that H4-TS does not appear to disrupt the π^* ordering of either PhH0-TS or PhH1-TS. The aromatic ordering of PhH0-TS displays a fairly linear increase as the fraction of aromatic is increased. This smooth transition suggests that PhH0-TS self-assembles in all compositions explored and that the degree of apparent ordering is purely a function of the amount of aromatic signal from the substrate. We propose that the ability of PhH0-TS to order as it does over a range of compositions in dense SAMs is a result of the molecule's structural rigidity. In contrast, PhH1-TS may actually display a slight increase in aromatic ordering in mixtures of H4-TS. The third aromatic, PhH2-TS, displays markedly different behavior in mixed systems of H4-TS. Specifically, the aromatic ordering in mixed systems of PhH2-TS and H4-TS is greatly reduced from that observed in the single-component SAMs and is much lower than that detected in mixtures of either of the other two aromatics. These data are consistent with a homogeneously blended system in which the PhH2-TS cannot organize through $\pi-\pi$ interactions of neighboring aromatic molecules and the flexible phenyl moiety extends beyond the neighboring short aliphatics.

The aromatic ordering trends observed in mixtures of H18-TS with either PhH0-TS or PhH1-TS are similar to those observed in mixtures involving H4-TS. This similarity suggests that the alkyl chain length has, at most, a small impact on the organization of the phenyl moieties of PhH0-TS and PhH1-TS, arguably owing to these molecules' bond angle constraints. Mixtures of H18-TS with PhH2-TS, however, show very different aromatic orientational trends than those of PhH2-TS with H4-TS. In the case of H4-TS mixtures, the phenyl moiety of the PhH2-TS is believed to extend beyond the short, neighboring alkyl chains, resulting in poor ordering of the phenyl rings. In mixtures of PhH2-TS with H18-TS, however, the phenyl groups are likely interspersed among long alkyl chains. This appears to produce an enhanced ordering of the phenyl moieties in mixtures of H18-TS. Additionally, whereas the ordering of the alkyl chains is still much less in mixtures with PhH2-TS than in pure films of H18-TS, the chain ordering in the mixtures with PhH2-TS does appear to be slightly greater than that observed for mixtures of H18-TS with PhH1-TS.

From these observations, it appears that neither the short (H4-TS) nor the long (H18-TS) trichlorinated aliphatic greatly affects the ordering of either of the two shortest aromatics (PhH0-TS and PhH1-TS); any apparent orientational changes in mixed systems are a consequence of the dilution of aromatic signal at higher aliphatic fractions. Both aliphatics do, however, appear to have an observable effect on the PhH2-TS—the H4-TS by disrupting PhH2-TS's ordering and the H18-TS by enhancing it.

Reflectance Fourier Transform Infrared Spectroscopy. Our NEXAFS measurements provided interesting information about the ordering competition between the phenyl group in PhH*x*-TS

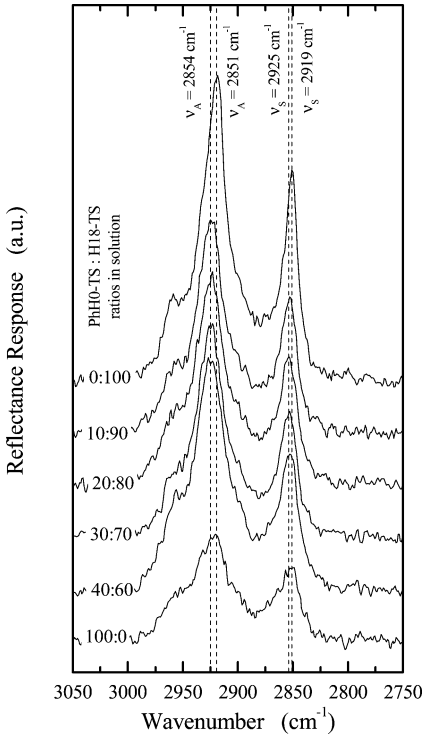

Figure 10. Reflectance FTIR responses for PhH0-TS/H18-TS mixtures of various compositions.

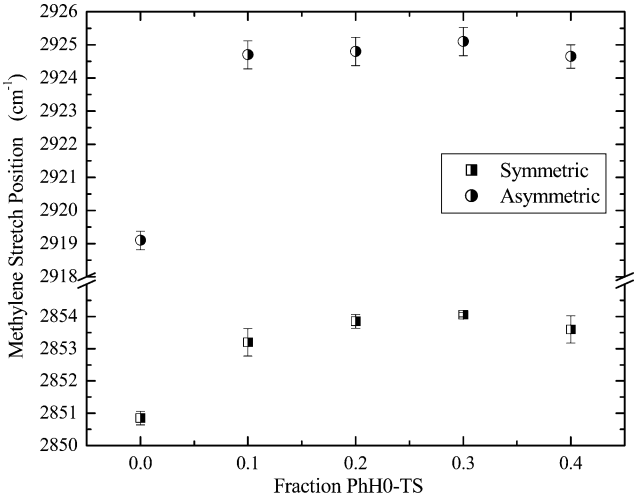

Figure 11. Average symmetric (■) and asymmetric (●) methylene stretching band positions. The shift in peak position upon the introduction of aromatic moieties is indicative of an increase in disorder of the aliphatic chains. The error bars denote one standard deviation.

and the alkyl chain in H18-TS (cf. bottom panel in Figure 9). We performed reflectance FTIR experiments in order to gain more insight into this behavior. The reflectance FTIR data were analyzed by using the ratio of the response from p-polarized light to that from s-polarized light and then subtracting the baseline curve. The resulting normalized spectra are presented in Figure 10. For SAMs of pure H18-TS, the asymmetric and symmetric methylene C−H stretches appear at 2919 and 2851 cm^{-1}, respectively. Earlier work of others established that the appearance of the methylene stretches at those two wavenumbers is a signature of a semicrystalline-like structure of the alkyl.[1,26,27] Upon adding a small amount (10% (w/w) total silane) of PhH0-TS to the deposition solution, these peaks shift to respective frequencies of 2925 and 2854 cm^{-1}. Additionally, the magnitudes of the peaks decrease with the addition of the aromatic component. Figure 11 details the positions of the symmetric and asymmetric methylene stretches as a function of the composition of the H18-TS/PhH0-TS mixed SAM. These changes in the peak attributes are a clear indication of at least partial loss of the semicrystalline arrangement of pure H18-TS.[1,26,27] These results are consistent with those observed from contact angle measurement and NEXAFS spectroscopy for mixed systems of H18-TS and PhH0-TS. They seem to indicate homogeneous blending of the two constituents rather than large-scale phase separation. What is clear is that a small amount of the aromatic constituent interspersed among the long-chain aliphatic disrupts the polymethylene chain ordering. It is not obvious, however, whether all alkyl chains get affected equally or whether there is still a small fraction of H18-TS present that maintains its original perpendicular orientation. Answering this question is not as straightforward as NEXAFS, which is perhaps the most sensitive of all of the tools that we use. NEXAFS measures only an "average" molecular orientation of the molecules because it averages all orientations in the beam-spot area (∼0.25 mm^2) on the sample. Hence, NEXAFS is incapable of discriminating between the cases involving all H18-TS molecules being homogeneously tilted by the same angle and the case of a partially disordered system with a broad distribution of tilt angles pointing into one average direction.

Conclusions

We have demonstrated through contact angle measurements on mixed systems of PhH0-TS and our four aliphatic species that bimolecular deposition solutions of PhH0-TS and a trichlorinated aliphatic result in a surface whose composition is closely related to the bulk solution composition. Hence, increasing the aromatic fraction in solution results in a tunable transition from primarily aliphatic to primarily aromatic on the surface. In contrast to this, solutions of PhH0-TS with a monochlorinated aliphatic produce surfaces whose compositions are preferentially aromatic when even relatively small amounts of PhH0-TS are mixed with large amounts of a monochlorinated aliphatic.

The results obtained from NEXAFS experiments are consistent with our contact angle data for PhH0-TS. The trend observed in the π^* resonance peaks over varying solution composition indicates a gradual transition in substrate coverage for mixed systems with trichlorinated aliphatics (H4-TS and H18-TS) and an abrupt transition to primarily aromatic surface coverage for mixed systems with monochlorinated aliphatics (H4-MS and H18-MS). This behavior is observed for all three of the aromatic species explored. Additionally, the presence of even a small amount of any aromatic constituent, when blended with long-chain aliphatics, disrupts polymethylene chain ordering. Whereas the orientation of the phenyl moieties on either of the two shortest aromatics (PhH0-TS and PhH1-TS) appears to be controlled primarily by the bond angles within the molecule, the orientation of PhH2-TS's phenyl moiety is greatly affected by the length of surrounding alky chains. This is because the PhH2-TS, unlike the other two aromatics explored, has sufficient mobility of the aromatic ring for its orientation to be influenced by intermolecular interactions.

Finally, we have corroborated through reflectance FTIR that small fractions of PhH0-TS will disrupt the ordering of H18-TS. This is a further indication that these molecules form a homogeneously blended system of aromatics and aliphatics in which no large-scale domain separation occurs. We have demonstrated that, in the case of mixed SAMs of trichlorinated aliphatic and aromatic silanes on silica, the resulting surface composition is tunable by controlling the composition of the

deposition solution. Systems including monochlorinated aliphatics in combination with trichlorinated aromatics, however, are not tunable because the monochlorinated species are incapable of adsorbing onto the surface competitively, suffer from the steric restrictions of their methyl substituents, and cannot take part in polysiloxane cross linking.

Acknowledgment. The work was supported by grants from the National Science Foundation (CTS-0403535) and the Office of Naval Research (N000140510613). NEXAFS spectroscopy experiments were carried out at the National Synchrotron Light Source, Brookhaven National Laboratory, which is supported by the U. S. Department of Energy, Division of Materials Sciences and Division of Chemical Sciences.

Supporting Information Available: Normalized 50° π^* peak height vs fraction of PhH1-TS and PhH2-TS in solution. C−C 1s → π^* and C−H 1s → σ^* 90° − 20° difference values for systems containing monochlorinated aliphatics. Ellipsometric and FTIR data. This material is available free of charge via the Internet at http://pubs.acs.org.

LA062475V